ADVANCED ENERGY MATERIALS
www.advenergymat.de

Dial-A-Particle: Precise Manufacturing of Plasmonic Nanoparticles Based on Early Growth Information—Redefining Automation for Slow Material Synthesis

*Bruno Pinho and Laura Torrente-Murciano**

Nanomaterials are at the core of many scientific discoveries in catalysis, energy and healthcare to name a few. However, their deployment is limited by the lack of reproducible and precise manufacturing technologies on-demand. In this work, a precision automated technology is demonstrated for nanoparticles synthesis with wide-range tunable sizes (≈4–100 nm). Dial-a-particle capabilities are achieved by a combination of a fast integrated multipoint particle sizing combined with a "plug-n-play" modular platform with reactors in series, distributed feed and in situ multipoint analysis. Real-time early growth information accurately predicts the resulting particle properties. Such real-time simple feedback control can overcome repeatability and stability issues associated with controllable (e.g., conditions) and uncontrollable (e.g., fouling, ageing, and impurities) variations leading to self-regulated, highly stable multistage systems with no human intervention even with long residence times (from a few minutes to hours). This is a paradigm shift from machine learning (ML) methodologies, which are restricted to trained networks with rich data sets, impractical in non-reproducible processes and limited to short residence times (e.g., within few minutes). The approach is demonstrated for plasmonic silver and gold nanoparticles showing agile control within minutes, opening the door for automation of more complex multistage procedures such as composites, multielement materials, and particle functionalization.

1. Introduction

Nanoparticles (NPs) discoveries are at the core of numerous scientific fields from catalysis, virology, hyperthermia, solar cells, drug delivery, stem cell, medical imaging, etc.[1–4] Their unique properties are strongly dependent on the chemical (e.g., composition, surface functionalization) and physical properties (e.g., size, shape). However, their potential and large-scale deployment are currently limited by the lack of continuous manufacturing technologies that combines precision, flexibility, and affordability.[1] In recent years, microreactors have emerged as powerful tools for the continuous synthesis of nanoparticles providing homogeneous conditions in terms of temperature and chemical environments thanks to their short mixing times and enhanced mass and heat transfer rates[2]. Both biphasic systems[3] and design of the reactor geometries in single-phase systems[4,5] have been explored to promote convection within the diffusion-dominated systems as a way of achieving homogeneous concentration profiles.[6]

Over the last years, the merits of automation have been successfully implemented in flow chemistry, especially for fast (i.e., < few minutes) organic transformations[7] and active pharmaceutical ingredients (APIs).[8] However, they have been applied to far less extend to nanomaterials synthesis[2,9,10] due to the slow (i.e., from tens of minutes to hours) and normally multistage synthesis required for the synthesis of materials with large dimensions (i.e., tens of nm) and complex structures (e.g., core–shell, multicomponent alloys). De Mello's group presented the first automated parameter optimization of nanoparticle synthesis in microfluidics[11] followed by a number of studies[12–17] accelerating multidimensional parameter screening. However, until now, such approach is only applicable to single-step fast synthesis and even though, they required a relatively large number of iterations to converge.[13–15] The optimization time expands considerably for systems dealing with slow reactions, which can spin out to weeks.[18] Another even bigger challenge is the fact that nanoparticle synthesis is affected not only by controllable parameters such concentration, temperature, dosing points, etc. but also by uncontrollable parameters such as fouling, ageing of solutions, batch-to-batch precursor variability, flow fluctuations, etc. making their manufacturing inherently irreproducible, unrepeatable and unstable. Indeed, our group has recently demonstrated the continuous synthesis of seed-mediated growth of silver citrate-based nanoparticles with sizes ranging from 4 to 80 nm. Despite being a technical breakthrough, the system still delivers an off-target inconsistency of >±13% when performing >100 characterized syntheses. Such inconsistency is associated not only to day-to-day variabilities but also irregularities during a continuous synthesis due to the abovementioned uncontrollable instabilities.

Dr. B. Pinho, Dr. L. Torrente-Murciano
Department of Chemical Engineering and Biotechnology
University of Cambridge
Philippa Fawcett Drive, Cambridge CB3 0AS, UK
E-mail: lt416@cam.ac.uk

The ORCID identification number(s) for the author(s) of this article can be found under https://doi.org/10.1002/aenm.202100918.

DOI: 10.1002/aenm.202100918

These systems are not suitable for artificial intelligence (AI) approaches since one would need to persistently recalibrate/retrain the neural network with extensive sets of non-repeatable data. Such limitations could be overcome by increasing the rate and quality of in-situ information generated, with integrated analytics recently emerging as powerful tools.[19] In this work, we push the boundaries of the field of automated synthesis of slow and complex materials. Herein, we present a real-time nanoparticle sizing and shape strategy integrated into modular flow systems through low-cost spectroscopy which enables fast (within few seconds) multipoint analysis, especially important in multi-stage syntheses. Such a powerful analytical tool underpins our dial-a-particle automation technology, which uses early growth information to mechanistically predict late particle properties through a simple single variable algorithm. The technology is demonstrated for large (i.e., multigrowth stages) silver and gold nanoparticles and it is easily applicable for the distributed manufacturing of materials on-demand with minor human intervention in a self-regulated manner driving material synthesis into the AI arena.

2. Manufacturing Platform

The novel manufacturing concept involves real-time access to information about the material synthesized at an early stage of the synthetic protocol, offering key data to predict the final material characteristics. The early access to data in long synthetic routes (above 10 min) is vital to ensure a smooth and simple operation with minor user-intervention beyond dial a particle size, define the plasmonic material of interest and prepare the required solutions. The platform hardware is based on a continuous multi-step plug-and-play process, where a series of continuous operations—material synthesis and characterization—are performed sequentially. Thanks to its modular nature and design, the overall structure is user-accessible, easily reconfigurable and fits in a small lab bench (1×1 m^2). The system's overall dimension is compact considering that each unit module integrates a set of diverse technologies: a mixer, a 3D microfluidic reactor, analytical characterization, cleaning/collecting valves and a heating module. It also compiles a set of process sections (**Figure 1**): a central control (computer and temperature PID controller), a chemical delivery station (syringe pumps and mass flowmeter), an analytical system (UV–Vis light source, spectrometer, optic multiplexer, optical fibers, optical flow cells and mass scale), an optical cleaning station (4-way valves and line) and a quenching/collection vessel.

Several technical challenges arose while implementing this novel multipoint real-time material characterization across the platform. First, physical properties such as light attenuation throughout the platform are considered (light source–multiplexer–flow cell–multiplexer–spectrometer) through careful design of optical cells and cleaning mechanism without disturbing the syntheses (Figure 1, 4-way valves). Finally, a mathematical algorithm is developed and calibrated (correction to dielectric function) to translate spectroscopy data to particle size, distribution and spherical degree. The spherical degree acts as a quality control parameter and it is defined by a quasi-spherical threshold, expressed by a low residual sum of squares between the experimental and theoretical spectra for spherical particles. The algorithm is based on Mie theory (analytical solution of Maxwell's equations for light scattering) initially applied for in situ characterization[4] and adapted here for in-line real-time inspection[4] (refer to Figure S3 and Tables S1 and S2, Supporting Information for more details). The in situ term was adopted because we are accessing intermediate points reactive points throughout the system.

The reactor design follows 3D helical microreactor configurations, which have been successfully applied to nanoparticle synthesis with narrow particle size distributions.[4,5] Helical type of reactors is 3D printed to achieve the desired flow pattern, as one can easily tune the recirculation vortices generated by centrifugal forces (Dean). They offer laminar flow patterns (i.e., low collision rate between particles), low mixing times and high transfer coefficients in comparison with batch or semibatch counterparts. This unique set of conditions aids the manipulation of nanomaterials in absence of organic capping ligands, with particles just stabilized electrostatically with reduced quantities of stabilizers such as trisodium citrate (weak stabilizer). Despite the reactors have a specific volume (1.36 mL), the range of residence times varies from, e.g., 11 to 5 min (R0 to R5) because of the sequential flow dosing (i.e., distributed feed). Please refer to Supporting Information for more details.

Tuning particle size over a wide range (5 to 100 nm) relies on separating fast nucleation and controllable growth, but also on maintaining an exquisite control over the concentration range in several reactors (Figure 1 for the synthesis of Ag). The synthetic approach follows a seed-mediated growth, which relies on the autocatalytic reduction of salts in the metal nanoparticle surface.[20,21] In a typical synthesis, particles are produced on the seed stage (R0) by mixing a strong reducing agent ($NaBH_4$) with a metal precursor (e.g., $AgNO_3$). This stage triggers rapid nucleation of small particles (e.g., ≈5 nm of ≈1.8E-6 m^2 Ag mL^{-1}) with narrow particle size distribution (<20%). $NaBH_4$:Ag ratio is optimized to ensure full consumption/degradation of $NaBH_4$ in the seed reactor.[5] Nucleation is followed by controllable growth using a mild reducing agent (e.g., trisodium citrate) over the growth stage (R1 to R5, Figure 1). The particle size (or growth rate) can be tuned by changing the number of growth reactors (R1 to R5) and the citrate to precursor ratio added in the growth stage. Please refer to Supporting Information for flow conditions and solution preparation.

The automated platform herein combines four layers of in-house developed software with graphical user interfaces (Figure S2, Supporting Information), compiling (i) instrument control, (ii) analytical acquisition, (iii) optimization, and (iv) particle characterization. A LabView code (i) monitors and controls multiple process parameters such as reactor temperature, flow rates, and total mass at the outlet. The MatLab code (ii) acquires time-reactor-resolved spectral information (full spectra, peak location, and optical density), and controls the multiplexer switching time between optical fibers. The optimization algorithm (iii) communicates in real time with the process control system LabView (i) to perform changes in the process by varying the inlet flowrate of metal precursor in

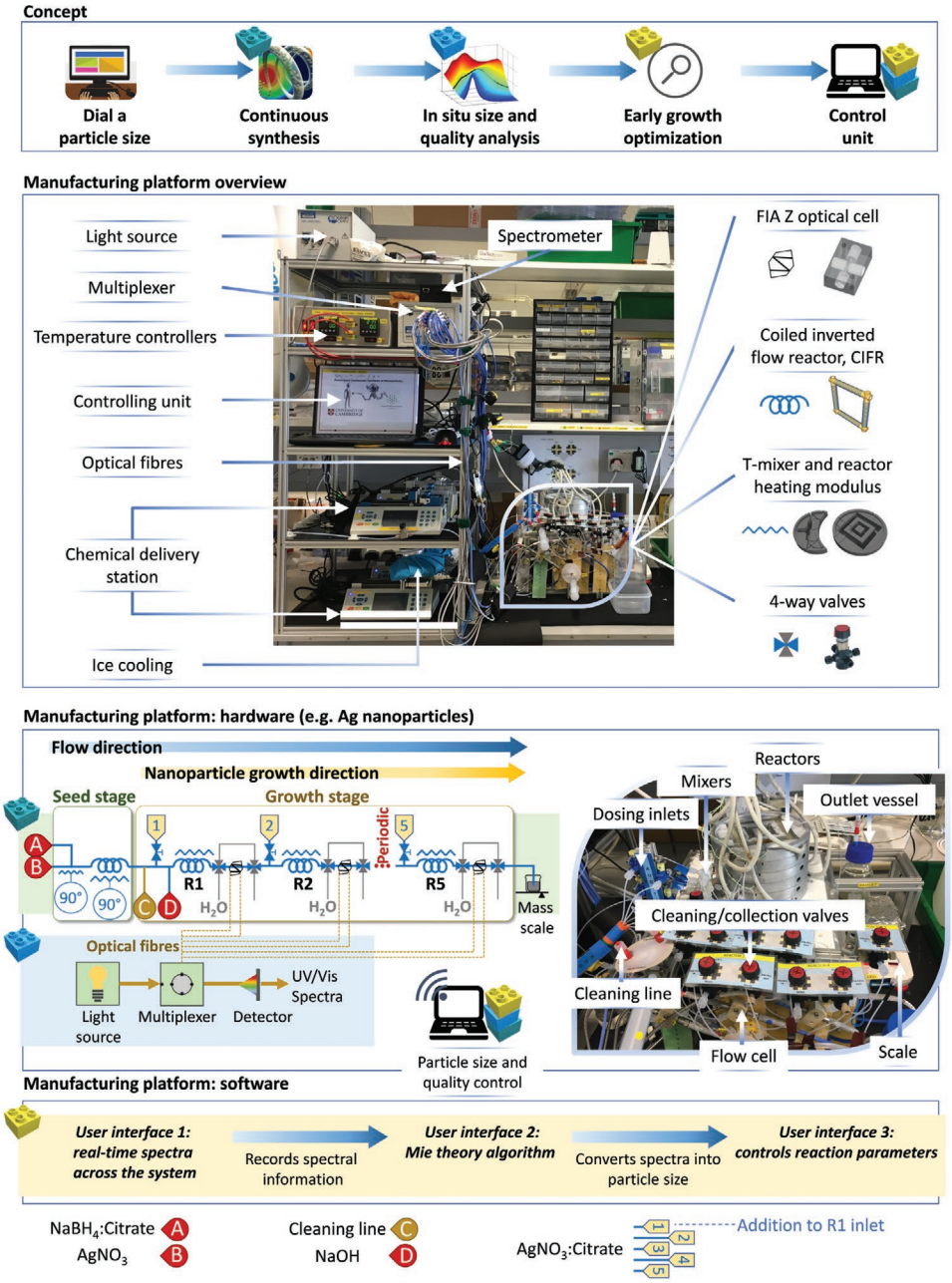

Figure 1. Self-optimized modular set-up with UV–Vis in situ analytics. The materials synthesis (hardware) is divided into two stages: seed and growth. In the growth stage, after each reactor, a set of optical flow cells allow high throughput screening (HTS). A multiplexer directs the light toward different flow cells, to be analyzed by a spectrometer. A graphic user interface (GUI) controls the system instruments: pumps, thermal PID controller, spectrometer, and mass scale. Another GUI monitors the spectra in all the reactors in real-time and controls the optimization process. Spectra are inspected for particle size using a Mie theory-based algorithm. All the software communicates with each other to achieve a self-optimized system (refer to the support information for extra details). Using heating modules and coiled flow inverted reactors (CFIR) helps to keep the system compact while controlling the fluid dynamics. Here the system has been applied to Ag, but it applies to other materials such as gold with minor changes (refer to Figure S1, Supporting Information). R1 to R5 represent the reactors in the growth stage.

the reactors which indirectly varies the local concentration of reacted and unreacted metal, localized ionic strength, and residence time. The optimization adopted was a 1D golden section search method, which proved to be adequate, dues to its low number of iterations and simplicity. A postprocessing code based on Mie theory (iv) is used to inspect nanoparticle sizes and spherical degrees (quasisphericity quality control). The Mie theory algorithm gives an average radius relative deviation of 11.5% for Ag and 4.9% for Au nanoparticles (comparing against TEM of commercial standards). A more detailed description of the system and Mie theory is provided in Figures S2 and S3 and Tables S1 and S2 (Support Information).

3. Dial-A-Particle Size Strategy: Control and Optimization

The slow (>10 min to ≈40 min) synthesis of materials with a wide range of sizes (5–100 nm) is highly sensitive toward a wide range of controllable and uncontrollable factors as mentioned before, being necessary to periodically adjusted the synthetic conditions accordingly. Normally, results can only be evaluated at the end (e.g., R5) after a full synthesis, one residence time (τ). Such feedback control approaches are slow. In addition, such a control strategy cannot cope with instability at the early stage of the synthesis. Other approaches, such as machine learning (ML) are impracticable for non-repeatable synthesis with long residence time synthesis (lack of analytical data) since neural networks would require periodic training (e.g., daily), which can be expensive and time-consuming. To handle these challenges, our unique approach uses a mechanistic understanding of the particle growth (predictive nature) and real-time validation. The algorithm sets the conditions to achieve the target size (e.g., R5) and acts at the early stage of the growing process (R1, ≈8 min) with an easy to implement feedback loop (**Figure 2**). This concept makes the system responsive, capable of mitigating instabilities and can be easily extrapolated to other metals (as demonstrated herein with silver and gold).

The first step of our strategy involves populating an initial database of conditions related to particle sizes with chemical conditions (reducing agent to precursor ratio, e.g., [citrate]:[$AgNO_3$]) with residence time (Figure 2A). This can be rapidly achieved using our rapid multipoint characterization with a Mie theory-based algorithm (priory calibrated), where it is possible to collect at least five points per experimental condition at a stationary state within minutes of operation. This throughput feature follows particle growth based on a single set of conditions without intermediate manual steps that compromise growth studies, such as agglomeration between synthesis, human error, etc.

The second step consists of applying a model to particle growth as a function of early growth (at R1) based on the data collected for the database. Size tunability and narrow size distribution require growth to be governed by size focusing, where metal ion reduction occurs at the surface of nanoparticles. This regime is ensured by keeping the ion concentration low enough (low supersaturation ratio) to limit primary nucleation but high enough to induce size focusing via diffusion-controlled growth with minimal role from Ostwald ripening.[22] Parametric studies on nanoparticle growth using $AgNO_3$ as a precursor and sodium citrate as a reducing agent reveal that [citrate]:[$AgNO_3$] should be between 0.5 and 100.[4] This set of experimental conditions define particle growth as $r^3 - r_0^3 = k\tau$ (Figure S6, Supporting Information), where r [nm] is the particle radius evaluated at a given time (τ), and r_0 [nm] is the seed particle radius, k [$nm^3\ min^{-1}$] is the growth rate and τ [s] is the

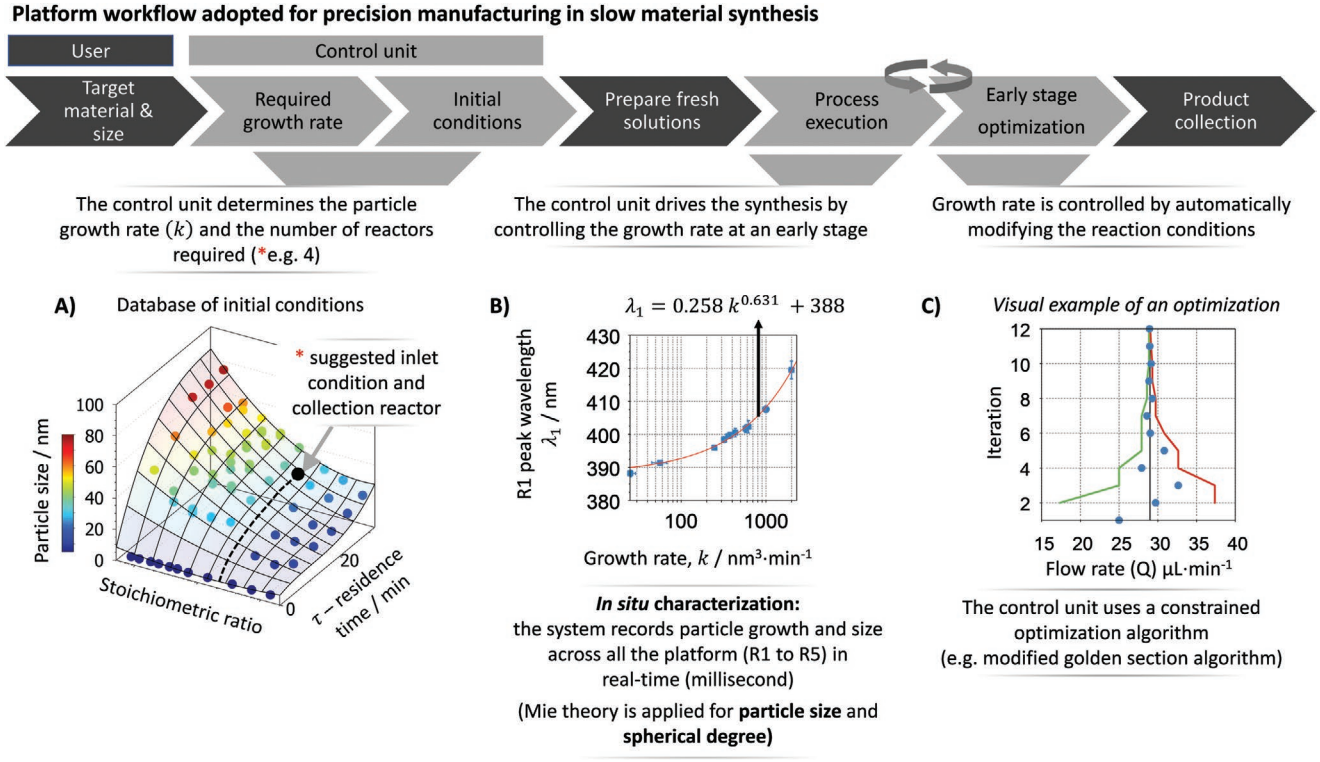

Figure 2. Optimization algorithm applied to nanoparticles synthesis (e.g., silver nanoparticles). A) Database relating [citrate]:[$AgNO_3$] ratio and residence time with particle size. These conditions cover a large set of growth rates (25 to 2000 $nm^3\ min^{-1}$) to be used as an initial guess for the optimization process. B) To measure the growth rate in real time (millisecond timescale), a relationship between peak wavelength at maximum absorption in R1 and growth rate is used. The data showing a constant growth rate across the system is presented in Figure S6 (Supporting Information) based on experimental results. C) The control and optimization of final particle size are based on a golden section algorithm, which uses early particle growth rate (e.g., at R1) to define reaction conditions. For additional information about the algorithm, refer to the Supporting Information.

residence time. By keeping the growth rate constant (refer to Figure S6, Supporting Information) and controlling the feed distributed through a series of reactors, the early growth (first growth reactor) can be translated to the outlet size of any of the reactor modules while facilitating a fast optimization. Therefore, the target growth rate can be translated into a target absorption wavelength using the correlation in Figure 2B. This is the core aspect of the self-optimized approach using in situ characterization.

The last step enables the optimization using a golden section-search due to its simplicity, no gradient and Hessian information necessary and confined interval of search. More robust methods such as gradient-based optimization can provide a fast convergence, but they require an extensive database. Here, it is of utmost importance to have an optimization method that converges with a minimum number of iterations. In each iteration, the flow rate of the distributed feed varies until the converge criteria is achieved. All the details about the optimization are detailed in Figure 2C.

4. Dial-A-Particle: 82 nm Silver

To demonstrate the automated manufacturing capabilities silver particles with a target size of 82 nm were synthesized. Such input information suffices for the algorithm to calculate the required growth ($2461\ nm^3/min^{-1} = ((82/2)^3 - (5/2)^3)/28$) and the number of reactors required, according to a defined residence time range limit per reactor. Then, using the database in Figure 2A, it estimates the initial [citrate]:[$AgNO_3$] ratio from a discrete range (or interpolated). In this case, the selected initial conditions normally lead to a growth rate of 1995 $nm^3\ min^{-1}$ using four reactors with fixed flow rate (refer to **Figure 3** caption). The optimization only acts when the system is in a stationary state at R1, and then it easily corrects the differences between the initial and required growth rate by changing flow rates of the dosing material at the growth stage. This translates into simultaneous changes in metal salt and reducing agent concentration and residence time (refer to Figure S7, Supporting Information for illustration of the combined effects on the particle growth). After triggering the optimization, the system requires about 95 min to achieve full stability across the different reactors (total residence time, $\tau \approx 30$ min). It is key to highlight that this approach makes the system agile, only requiring a total optimization time below the standard 3τ in flow chemistry to reach a stationary state[23] and thus, decreasing time and waste. This stabilization time can be decreased if one reduces: the target size, number of rectors and sources of instabilities (bubbles). In addition to particle size, the Mie theory-based algorithm provides additional information about the shape quality during synthesis. Spherical silver nanoparticles with a size of 82.2 nm were achieved within just three iterations as shown in Figure 3.

5. Manufacturing Stability and Quality Control

Stability during synthesis is a critical factor in continuous multi-step material manufacturing, and it accounts for uncontrollable time-dependent changes across the sequence of reactors, such as fouling, ageing of stock solution, bubble formation, etc. This factor is a parameter often disregarded, but it needs to be accounted for if the manufacturing platform run for long periods (hours/days). In this case, the system's stability can be evaluated thanks to the rapid acquisition of multi-reactor spectroscopy data which provides time-resolved data throughout the synthesis. The particle size distribution and spherical degree were evaluated over a long experimental time, 250 min (**Figure 4**). The results here presented are obtained after an initial optimization process (no further mitigation of instabilities) targeting 82 nm with a relaxed convergence criterion. The time-averaged particle size was evaluated as 55.9 (R1) and 79.9 (R4) with 4.4 and 5.4 nm variations respectively. The gross majority of the particles synthesized corresponded to quasi-spherical/spherical particles; quality control represented by the threshold RSS≤0.4. These results represent the first success for a stable, complex, multistep material synthesis, fully characterized in real-time and precise, without the presence of surfactants and other mitigation protocols, such as reducing the bubble formation with a back-pressure regulator, etc.

6. Dial-A-Particle: 23 and 55 nm Silver

Meeting production demands to tune particle size can be accomplished through simple adjustments. The platform can be easily reconfigured to cater to a wide range of particles from ≈5 nm in the seed reactor (R0) to > 80 nm with five growth reactors. To illustrate the process, the transition from a target particle size of 82 to 55 nm only requires a new estimation of the new growth rate and minimum user intervention to vary the concentration of solutions as estimated by the algorithm (**Figure 5**). The required growth rate for 55 nm particles is estimated to be $742\ nm^3/min^{-1}$ [$k = ((55/2)^3 - (5/2)^3)/28$]. The system requires only ≈75 min (five interactions) to reach the required growth rate (corresponding to a spectral location at R1) and ≈100 min to reach stability across all the reactors (user-defined convergence constraints at 1 nm). For particles sizes below ≈25 nm, tunability of the growth rate is coarse at high pH values (e.g., 12) and low seed concentration being necessary to manipulate such parameters.[21] For lower ranges of sizes, the hydrodynamics plays a more significant role than concentration. The required growth rate for 23 nm particles is estimated to be $72\ nm^3/min^{-1}$ [$k = ((23/2)^3 - (5/2)^3)/21$]. The system needed ≈70 min (four interactions) to reach the required growth rate (corresponding to a spectral location at R1), and ≈90 min to reach stability across all the reactors (user-defined convergence constraints at 1 nm), reaching a final size of 23.8 nm. These results demonstrate that the system can meet size demand easily in a reasonable time, without mathematical complications.

For 23 nm, the starting conditions selected by the algorithm were: [citrate]:[$AgNO_3$] ratio of 14×10^{-3} M:0.1×10^{-3} M, $[NaOH]_{IN}$ of 0×10^{-3} M, 90 °C. The initial flow rates of each stream are (refer to Figure 1): 62.5 µL min^{-1} for (A), 62.5 µL min^{-1} for (B), 0 µL min^{-1} for (D) and 10 µL min^{-1} for (1 to 5). The seeds were

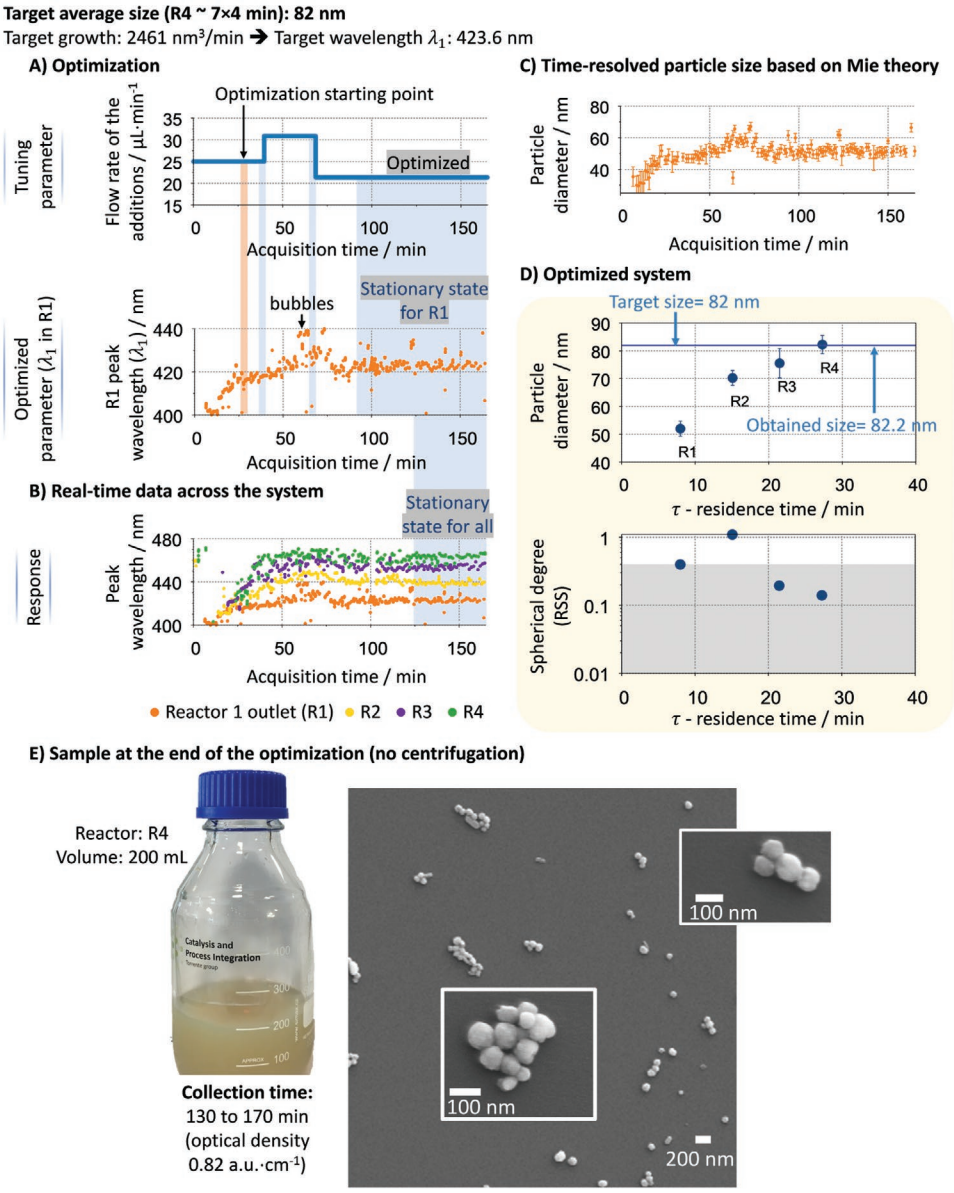

Figure 3. Optimization example to obtain silver nanoparticles sizes of 82 nm (the control unit estimates a target growth rate of 2461 nm^3 min^{-1} starting with seeds of 5 nm, corresponding to a target peak wavelength of 423.6 nm at the outlet of R1). A) Time-resolved results for the tuning parameter (inlet flow rate in the growth reactors) and its effect on the peak location in R1 (controlled parameter). B) Peak wavelength location across the system (R1 to R4). C) Calculated particle sizes on R1 during optimization with their respective size distribution represented in error bars based on the Mie theory algorithm. D) Resulting particle sizes and shape control parameter at the end of the optimization process. E) SEM picture of the resulting Ag nanoparticles. The left photo shows 200 mL of silver nanoparticles with an optical density of 0.82 a.u. cm^{-1} collected over 40 min. Initial conditions: [citrate]:[$AgNO_3$] ratio of 3.5×10^{-3} M:4.0×10^{-3} M, [NaOH] = 60×10^{-3} M, 90 °C. The initial flow rates of each stream are (refer to Figure 1): 62.5 µL min^{-1} for inlet A and B and, 25 µL min^{-1} for inlet D and inlets 1 to 4).

made at the seed stage using 50×10^{-6} M $AgNO_3$, 350×10^{-6} M citrate, and 25×10^{-6} M $NaBH_4$.

For 55 nm, the starting conditions selected by the algorithm were: [citrate]:[$AgNO_3$] ratio of 7×10^{-3} M:4×10^{-3} M, $[NaOH]_{IN}$ of 60×10^{-3} M, 90 °C. The initial flow rates of each stream are (refer to Figure 1): 62.5 µL min^{-1} for (A), 62.5 µL min^{-1} for (B), 25 µL min^{-1} for (D) and 25 µL min^{-1} for (1 to 5). The seeds were made at the seed stage using 1×10^{-3} M $AgNO_3$, 20×10^{-3} M Citrate and 3×10^{-6} M $NaBH_4$.

7. Repeatability

System repeatability is key to meet customer's demands over different batches. In the materials supply industry, it is key for the companies' reputation. Our unique approach to optimize early growth rate as a way of predicting the final particle size provides high accuracy (5.5% of average relative deviation) in achieving the target size across the whole size range (≈4–100 nm) without day-to-day variability, demonstrating the advantages of the automated

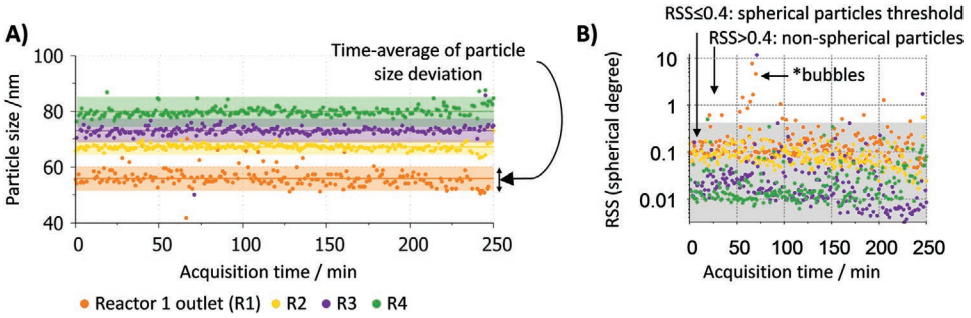

Figure 4. System's stability during a long-experimental run for the synthesis of silver nanoparticles (target size of 82 nm) with four growth reactors in series. A) particle size and B) RSS (spherical degree), which is the residual sum of squares between the theoretical spectrum of a spherical particle and the experimental one[4]). (*) The sporadic formation of bubbles modifies the flow pattern, leading to particle-to-particle interaction and the formation of nonspherical particles (RSS > 0.4). The particle sizes and their standard deviations were calculated using a Mie theory-based algorithm.

system. On the other hand, without such feedback approach, day-to-day discrepancies on the initial particle size and peak location (R1) leads to measurable variations (13% of average relative deviation with large dispersion outside 20% line) on the final particle size (**Figure 6**A). The reasons for the variability, mitigated by our real-time optimization approach are related to nonconformities: i) in the number of seeds, ii) sample preparation, iii) presence of undetected fouling, iv) stock solution degradation, etc.

8. Dial-A-Particle: 55 nm Gold

In this section, we show the adaptability of this approach to other plasmonic materials, such as gold nanoparticles. The only requirement is to ensure that particles growth follow a model (linear or nonlinear). In this case, the conditions were set to have linear growth, a characteristic favored by the lack of capping ligands during the synthesis. To perform real-time

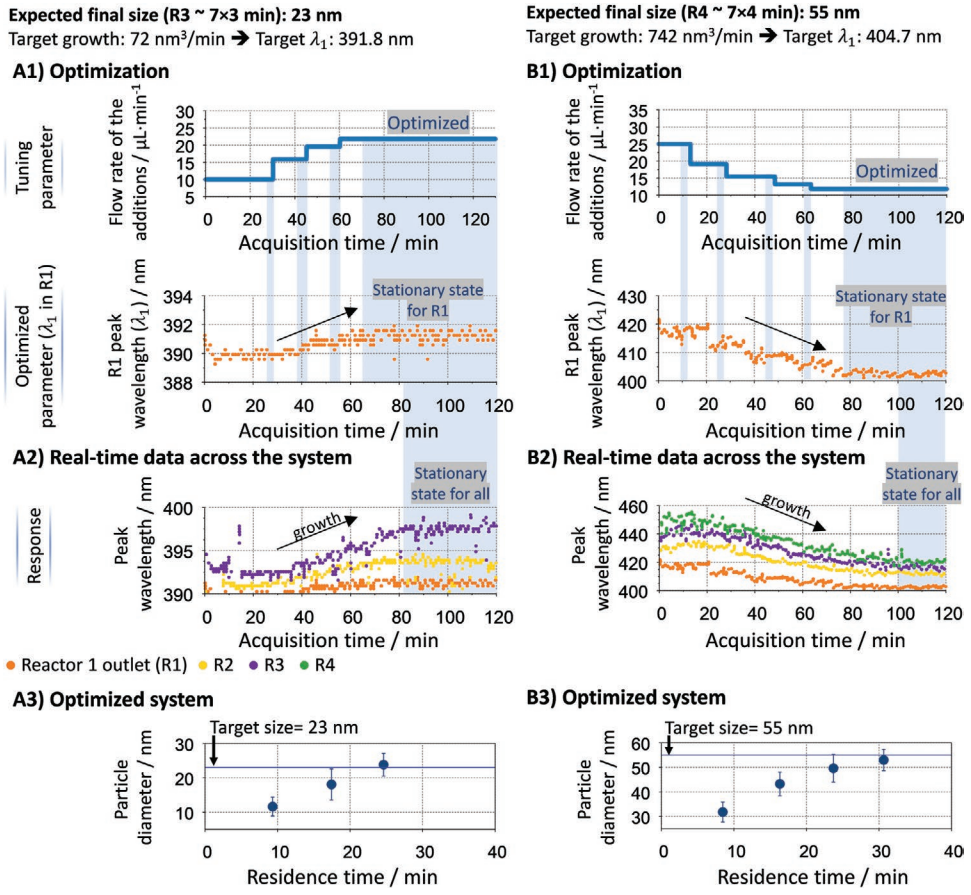

Figure 5. Optimization examples to obtain silver nanoparticles of 23 and 55 nm (the control unit estimates a target growth rate of 72 and 742 nm^3 min^{-1}, respectively, corresponding to a target peak wavelength of 391.8 and 404.7 nm). A1–B1) Time-resolved results for the tuning parameter (inlet flow rate in the growth reactors) and its effect on the peak location in R1 (controlled parameter). A2–B2) Wavelength location across the system. A3–B3) Calculated particle sizes on R1 during optimization with their respective size distribution represented in error bars based on the Mie theory algorithm.

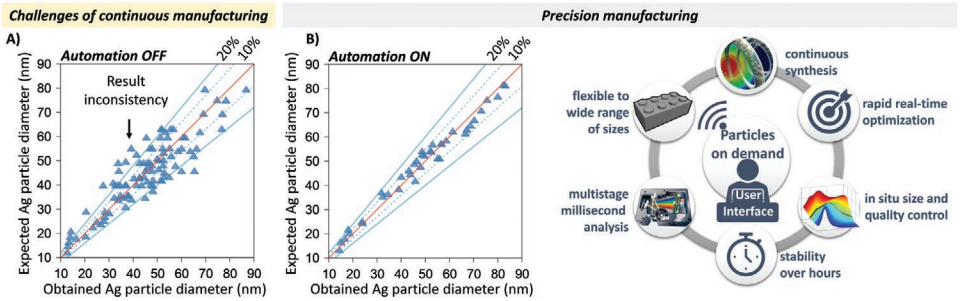

Figure 6. A) Results inconsistency for multistage nanoparticle manufacturing covering more than 100 syntheses with a wide range of sizes and no automation protocol. The average relative deviation is ±13% between the obtained and expected particle diameter. B) To diminish inconsistencies, a novel concept of precision manufacturing is adopted, being compromised in six fundamental modules with minimal human intervention. The target size is achieved with precision and excellent repeatability when the automation is on. The average relative deviation is ±5.5% between the obtained and expected particle diameter The particle sizes were calculated using a calibrated Mie theory algorithm applied to the spectra. Two examples of the acquired time-resolved raw spectra can be found in Figure S5 (Supporting Information).

optimization an initial database for particle size as a function of citrate to $HauCl_4$ ratio is required (refer to **Figure 7**A). To illustrate the process, a 55 nm particle of gold was targeted using the self-optimized manufacturing system, requiring a growth rate of 716 nm^3 min^{-1} (R4). Similar to the synthesis of the silver nanoparticles, the initial set of experimental conditions (citrate:$HauCl_4$) with values close to the growth rate required is estimated by the algorithm, Figure 7A. Gold nanoparticles with a size of ≈53 nm were achieved in ≈75 min with a relaxed convergence criterion. For the time-analyzed after optimization, the system remains stable for at least 40 min without performance degradation (Figure 7B). The results demonstrate that our multistage platform can be applied to other plasmonic materials with simplicity and with barely any changes in the configuration, being a highly desirable feature in any manufacturing platform.

9. Conclusions

Until now, multistep continuous material manufacturing was limited by the instability and unrepeatability caused by a large number of uncontrollable parameters such as fouling and stock ageing leading to off-target inaccuracies of ≈15%. This work overcomes such issues showcasing an automation approach with real-time control where real-time monitoring and early growth optimization leads to the precise and on-target control over the whole production time. The technology is showcased in a dial-a-particle fashion for the continuous synthesis of gold and silver particles with tunable sizes over a wide range (≈2–100 nm). To achieve this we combined several aspects: i) a "plug-n-play" platform with microreactors connected in series (previous approaches normally use a single reactor) and distributed feed across the different reactors to keep the concentrations of the reagents within certain limits to avoid parallel phenomena (i.e., Ostwald ripening), ii) an integrated characterization strategy using low-cost online spectroscopy, coupled with a Mie-theory based algorithm to provide real-time information of the size and shape of the nanoparticles. Such real-time rapid feedback control allows, for the first time, a self-regulated system to mitigate the interferences of the abovementioned uncontrollable parameters in systems with long residence times (tens of minutes to hours) without human intervention. The resulting system is capable of achieving a target size within a few nanometers in just 2–3 residence time. The approach can be directly extrapolated to other plasmonic materials, such as quantum dots, perovskites,

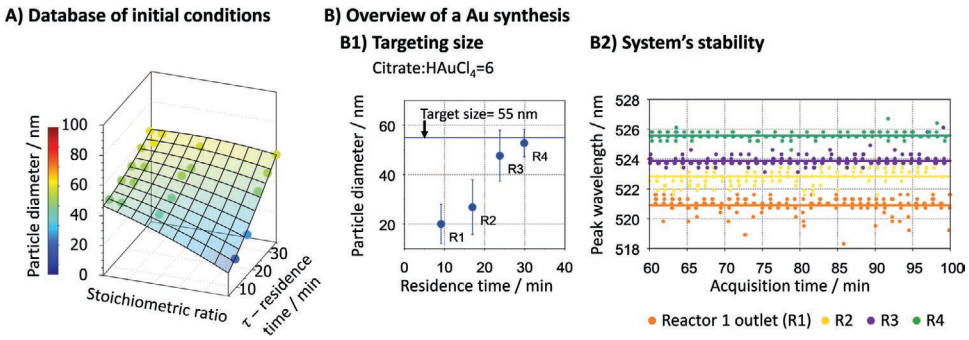

Figure 7. A) Database of experimental conditions relating [Citrate]:[$HAuCl_4$] ratio and residence time with particle size. B) Optimization results to obtain gold nanoparticles with a target size of 55 nm (the control unit estimates a target growth rate of 716 nm^3 nm^{-1}). The multimodular system for this synthesis of gold is shown in Figure S2 (Supporting Information). B1) Calculated particle sizes at a stationary state achieved at the end of the optimization. B2) Time-resolved gold nanoparticles stability across the system using peak wavelength (Citrate:$HAuCl_4$ = 6). The data was acquired from the reactor outlet 1 to 4 (R1 to R4). The spectral raw data for the experiment present on (B) for gold nanoparticles can be found in Figure S8 (Supporting Information). The particle sizes and their standard deviations were calculated using a Mie theory algorithm.

aluminum, etc. It probes the concept of automation for multi-stage, long (few minutes to hours) processes, paving the way to automated, precise material manufacturing with low production cost and minimum chemical waste.

Supporting Information

Supporting Information is available from the Wiley Online Library or from the author.

Acknowledgements

The authors greatly acknowledge the financial support from UK Engineering and Physical Science and Research Council (grant number EP/L020443/2).

Conflict of Interest

The authors declare no conflict of interest.

Data Availability Statement

Research data are not shared.

Keywords

automated systems, flow synthesis, plasmonic particles, self-regulated systems

Received: March 19, 2021
Revised: June 1, 2021
Published online:

[1] *Global Nanoparticles Market in Biotechnology and Pharmaceutical Sectors, 2017–2021*, **2017**, https://www.researchandmarkets.com/reports/4430360/global-nanoparticles-market-in-biotechnology-and (accessed: January 2021).

[2] S. Marre, K. F. Jensen, *Chem. Soc. Rev.* **2010**, *39*, 1183.
[3] C.-X. Zhao, A. P. J. Middelberg, *Chem. Eng. Sci.* **2011**, *66*, 1394.
[4] B. Pinho, L. Torrente-Murciano, *React. Chem. Eng.* **2020**, *5*, 342.
[5] K.-J. Wu, G. M. De Varine Bohan, L. Torrente-Murciano, *React. Chem. Eng.* **2017**, *2*, 116.
[6] Y. Gao, B. Pinho, L. Torrente-Murciano, *Curr. Opin. Chem. Eng.* **2020**, *29*, 26.
[7] D. E. Fitzpatrick, S. V. Ley, *Tetrahedron* **2018**, *74*, 3087.
[8] A. Adamo, R. L. Beingessner, M. Behnam, J. Chen, T. F. Jamison, K. F. Jensen, J.-C. M. Monbaliu, A. S. Myerson, E. M. Revalor, D. R. Snead, T. Stelzer, N. Weeranoppanant, S. Y. Wong, P. Zhang, *Science* **2016**, *352*, 61.
[9] S. Sevim, A. Sorrenti, C. Franco, S. Furukawa, S. Pané, A. J. deMello, J. Puigmartí-Luis, *Chem. Soc. Rev.* **2018**, *47*, 3788.
[10] J. Nette, P. D. Howes, A. J. deMello, *Adv. Mater. Technol.* **2020**, *5*, 2000060.
[11] S. Krishnadasan, R. J. C. Brown, A. J. deMelloa, J. C. deMello, *Lab Chip* **2007**, *7*, 1434.
[12] S. Li, R. W. Baker, I. Lignos, Z. Yang, S. Stavrakis, P. D. Howes, A. J. deMello, *Mol. Syst. Des. Eng.*, **2020**, *5*, 1118.
[13] L. Bezinge, R. M. Maceiczyk, I. Lignos, M. V. Kovalenko, A. J. deMello, *ACS Appl. Mater. Interfaces* **2018**, *10*, 18869.
[14] R. W. Epps, K. C. Felton, C. W. Coley, M. Abolhasani, *Lab Chip* **2017**, *17*, 4040.
[15] K. Abdel-Latif, R. W. Epps, C. B. Kerr, C. M. Papa, F. N. Castellano, M. Abolhasani, *Adv. Funct. Mater.* **2019**, *29*, 1900712.
[16] H. Bolze, P. Erfle, J. Riewe, H. Bunjes, A. Dietzel, T. P. Burg, *Micromachines* **2019**, *10*, 179.
[17] A. A. Volk, R. W. Epps, M. Abolhasani, *Adv. Mater.* **2021**, *33*, 2004495.
[18] D. L. A. Fernandes, C. Paun, M. V. Pavliuk, A. B. Fernandes, E. L. Bastos, J. Sá, *RSC Adv.* **2016**, *6*, 95693.
[19] J. Nette, P. D. Howes, A. J. deMello, *Adv. Mater. Technol.* **2020**, *5*, 2000060.
[20] K.-J. Wu, L. Torrente-Murciano, *React. Chem. Eng.* **2018**, *3*, 267.
[21] N. G. Bastús, F. Merkoçi, J. Piella, V. Puntes, *Chem. Mater.* **2014**, *26*, 2836.
[22] N. G. Bastús, J. Comenge, V. Puntes, *Langmuir* **2011**, *27*, 11098.
[23] H. S. Fogler, in Elements of Chemical Reaction Engineering, 4th ed., *Prentice-Hall International Series in the Physical and Chemical Engineering Sciences* (Ed: N. R. Amundson), Prentice Hall PTR, Upper Saddle River, NJ **2006**, p. 957.